a

Patient ID	Sex	Age	Pathology	MGMT Status	Prior Treatment	WES Regions	Custom-Capture Regions	RNA-Seq Regions	TCR Seq Regions
GBM030	M	57	*IDH1* WT GBM	Methylated	N	2	2	2	--
GBM032	M	42	*IDH1* WT GBM	Methylated	N	4	4	3	4
GBM051	M	53	*IDH1* WT GBM	Unmethylated	N	3	3	3	--
GBM052	M	79	*IDH1* WT GBM	Unmethylated	N	3	3	2	3
GBM055	F	82	*IDH1* WT GBM	Unmethylated	N	3	3	1	3
GBM056	F	55	*IDH1* WT GBM	Unmethylated	N	3	3	3	3
GBM059	F	66	*IDH1* WT GBM	Unmethylated	N	3	3	1	3
GBM062	F	49	*IDH1* R132H GBM	Methylated	N	3	3	3	3
GBM063	M	55	*IDH1* WT GBM	Unmethylated	N	3	3	3	2
GBM064	F	55	*IDH1* WT GBM	Unmethylated	N	3	3	3	2
GBM069	M	70	*IDH1* WT GBM	Methylated	N	3	1	3	--
GBM070	F	61	*IDH1* WT GBM	Methylated	N	3	3	2	3
GBM074	M	51	*IDH1* WT GBM	Unmethylated	N	3	3	3	3
GBM079	M	66	*IDH1* WT GBM	Unmethylated	N	3	3	3	3
AO083	F	37	*IDH1* R132H Anaplastic Oligo.	N/A	N	3	3	3	3
GBM018.Re	F	59	*IDH1* WT GBM	Unmethylated	TMZ, XRT	3	3	3	--
GBM031.Re	M	55	*IDH1* WT GBM	Unmethylated	TMZ, XRT	4	4	4	--
GBM047.Re	M	51	*IDH1* WT GBM	Unmethylated	TMZ, XRT, Optune	3	3	2	3
GBM065.Re	M	25	*IDH1* R132H GBM	Indeterminate	PCV, TMZ, XRT	4	2	2	2

b

Patient ID	Sex	Age	Pathology	Prior Treatment	WES Regions	Custom-Capture Regions	RNA-Seq Regions	TCR Seq Regions
BrMET008	M	81	NSCLC	Carboplatin, Pemetrexed	4	4	4	4
BrMET009	M	58	NSCLC	N	3	3	3	3
BrMET010	F	60	NSCLC	N	3	3	3	3
BrMET018	F	57	Breast	Taxol	3	3	3	3
BrMET019	F	59	SCLC	N	3	3	3	3
BrMET023	F	48	Breast	Carboplatin, Taxotere, Abraxane, Herceptin/Perjeta	3	3	3	--
BrMET024	F	59	Breast	TDM1, Docetaxel, Capecitabine, Tamoxifen, Exemestane, Herceptin	3	3	3	--
BrMET025	F	71	NSCLC	N	3	3	2	3
BrMET027	F	31	Breast	Carboplatin, Taxotere	3	3	3	3
BrMET028	M	69	Melanoma	N	3	3	3	3
BrMET058	F	54	NSCLC	N	2	2	1	--

Supplementary Fig. 1: Clinical details of study cohort. Clinical and study-specific details for glioma (a) or BrMET (b) patients included in the work. The number of spatially distinct regions from each tumor that underwent a given analysis is indicated in the last four columns. NSCLC - Non-small cell lung cancer. SCLC - Small cell lung cancer. MGMT - O-6-methylguanine-DNA methyltransferase.
WES - Whole-exome sequencing. TMZ - Temozolomide. RT - radiotherapy. PCV - procarbazine, lomustine (CCNU), vincristine.

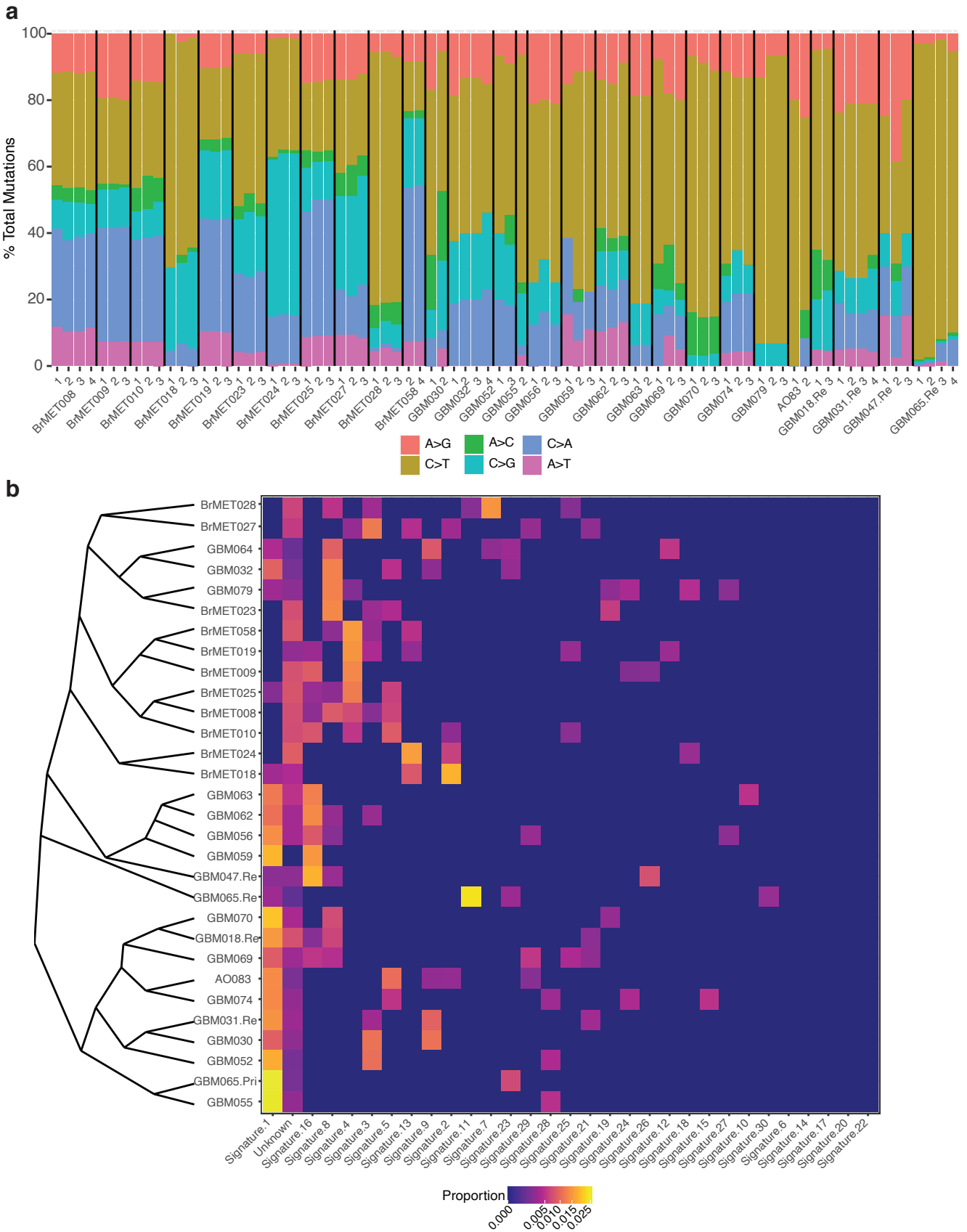

Supplementary Fig. 2: Mutational spectrum and signatures across cohort. a, Spectrum of single-nucleotide variants across cohort. **b**, Distribution of mutational signatures across cohort generated by deconstructSigs. Signature descriptions at http://cancer.sanger.ac.uk/cosmic/signatures.

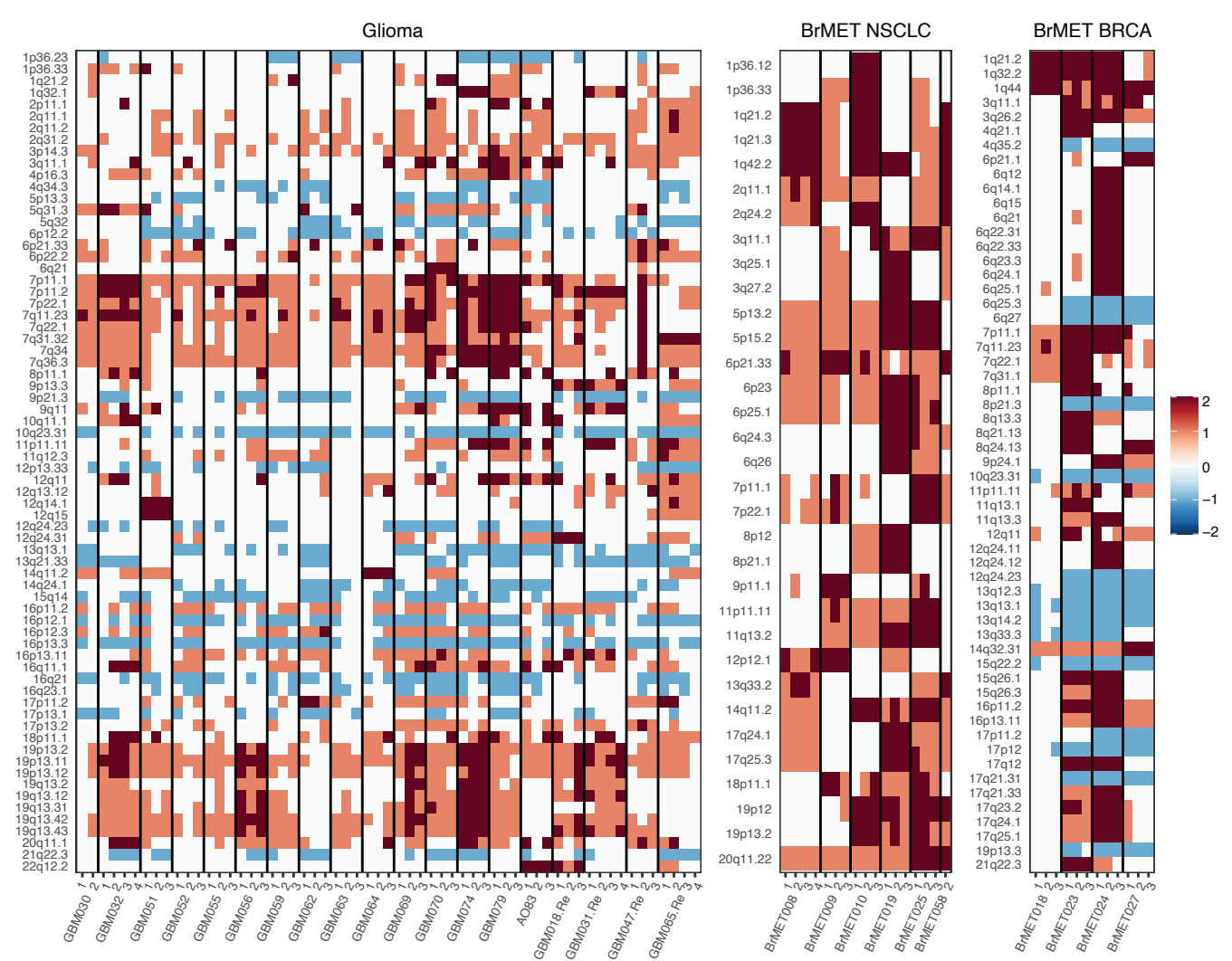

Supplementary Fig. 3: Intratumoral landscape of recurrent copy number variation events. Copy number variation events in gliomas (left), non-small cell lung cancer brain metastases (middle) or breast cancer brain metastases (right). Colors depict relative intensity of copy number alterations per sample. Positive scores in red indicate amplifications and negative scores in blue indicate deletions.

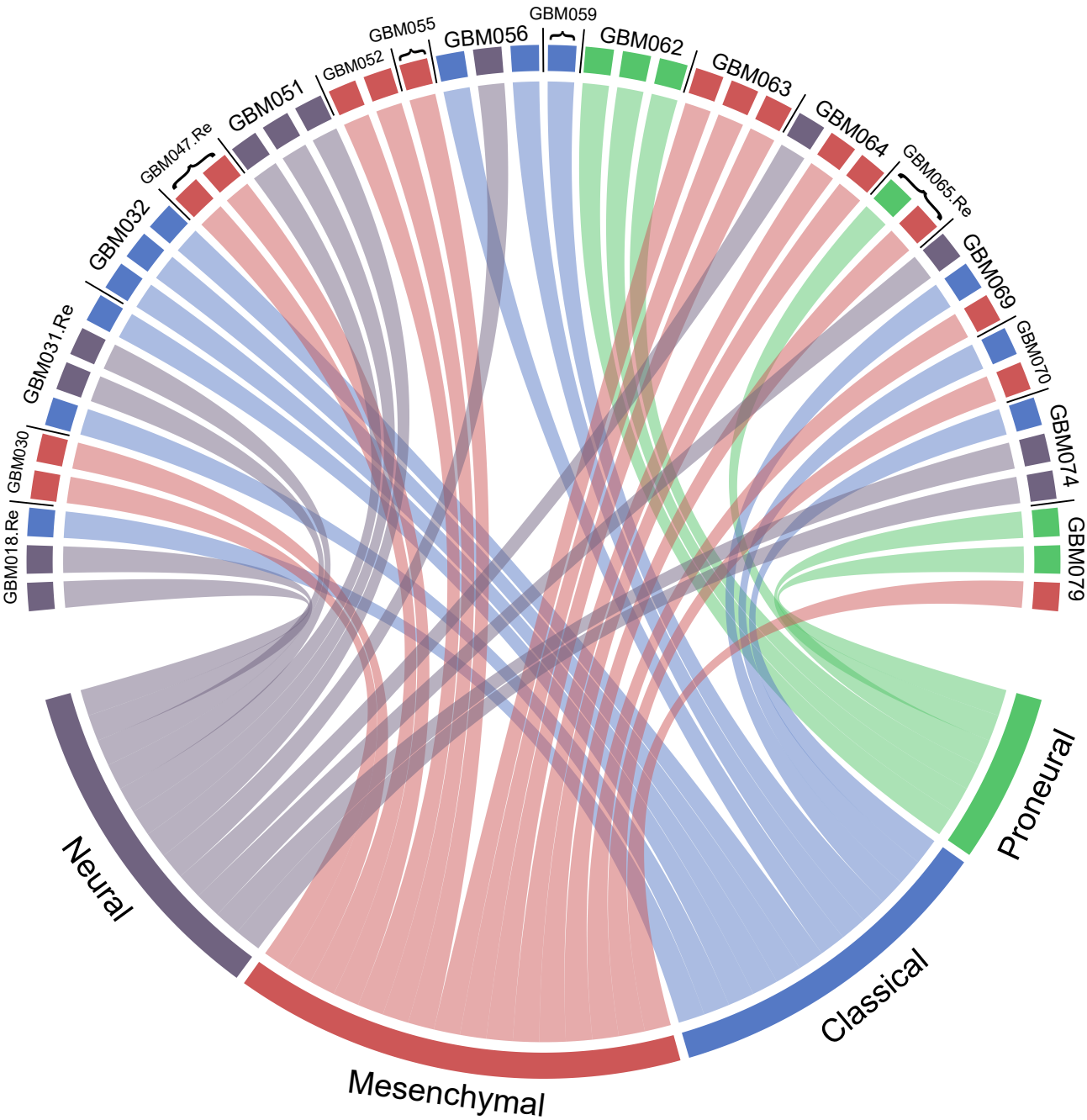

Supplementary Fig. 4: Molecular subtype classification of GBM. Circos plot displaying the classification of each tumor region among the four molecular subtypes of GBM. Classification was determined by gene set enrichment analysis on previously defined gene signatures (see Methods).

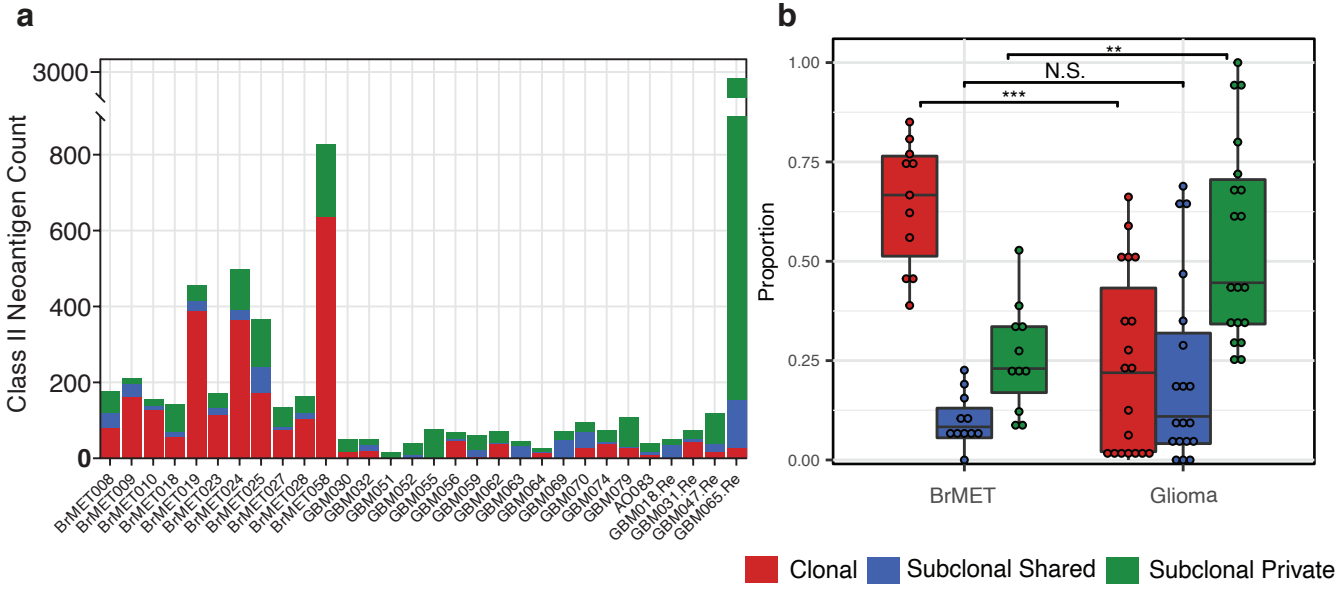

Supplementary Fig. 5: Class II neoantigen clonality. a, Class II neoantigen clonality per tumor. **b**, Proportion of clonal, subclonal shared, and subclonal private class II neoantigens in brain metastases and gliomas. Significance determined by unpaired t-test. **p< 0.01, ***p< 0.001.

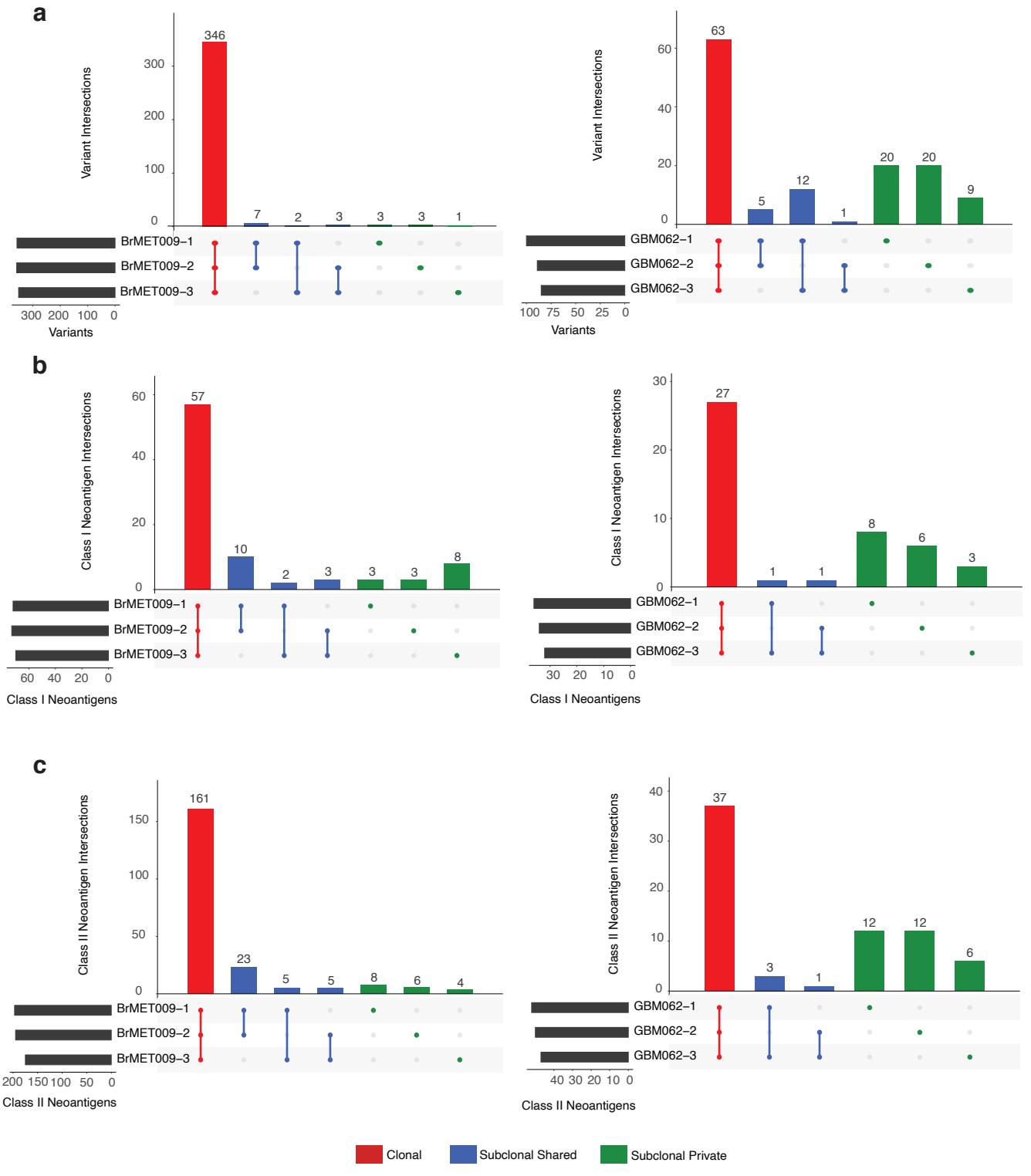

Supplementary Fig. 6: Spatial distribution of variants and neoantigens. Spatial distribution of variants **(a)**, class I neoantigens **(b)**, and class II neoantigens **(c)** for two represenative examples. Variants/neoantigens are grouped based upon the set of tumor regions in which they are shared.

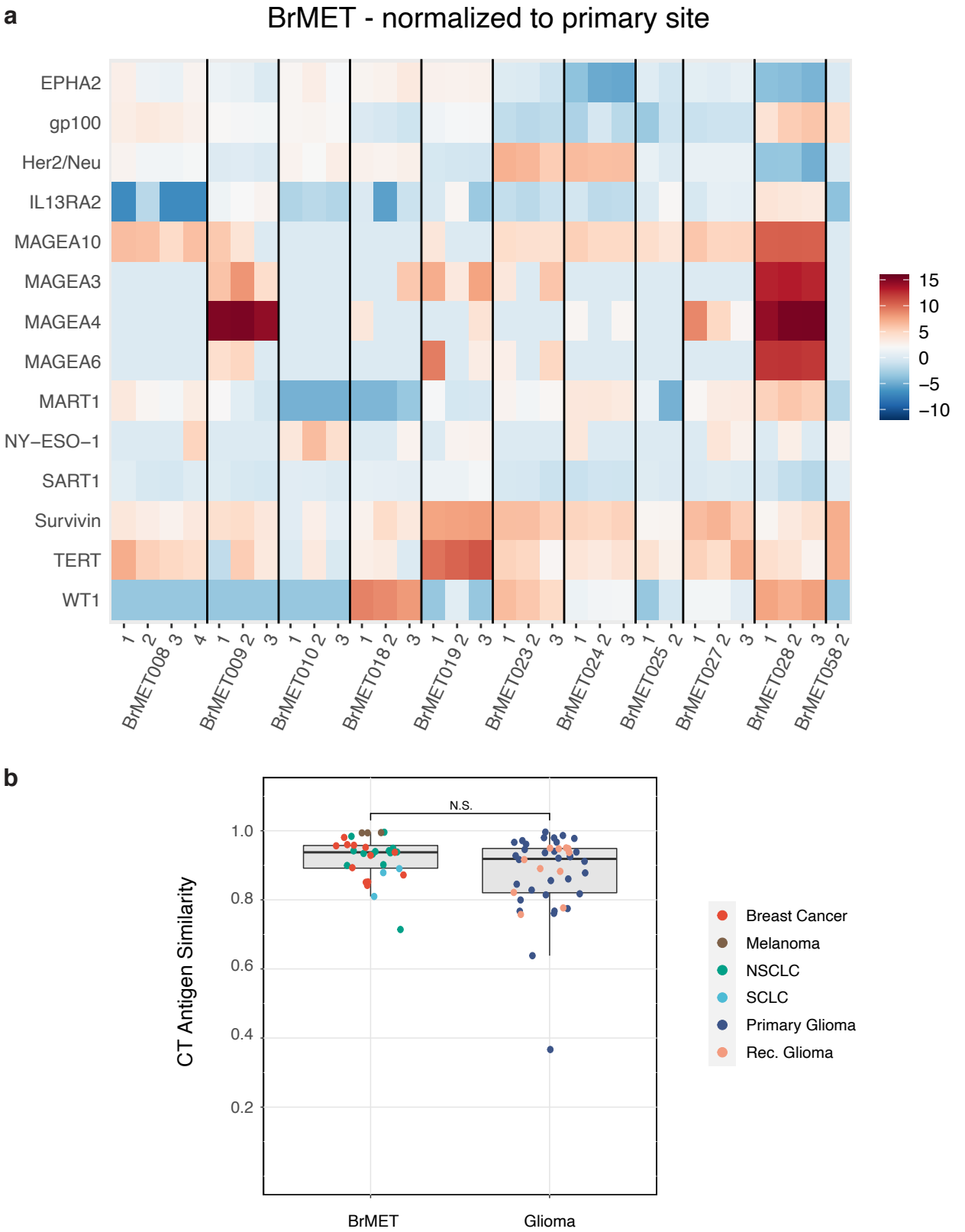

Supplementary Fig. 7: Intratumoral cancer/testis antigen similarity. a, Heat map of cancer/testis (CT) antigen scores for each BrMET tumor sample calculated by normalizing tumor expression to matched primary tissue site expression for each gene (in contrast to "Brain-Cortex" expression as done in Fig. 3).
b, Comparison of intratumoral CT antigen similarity as assessed by a pairwise cosine similarity metric on vectors composed of the scores (normalized to "Brain-Cortex" expression) for each CT antigen.

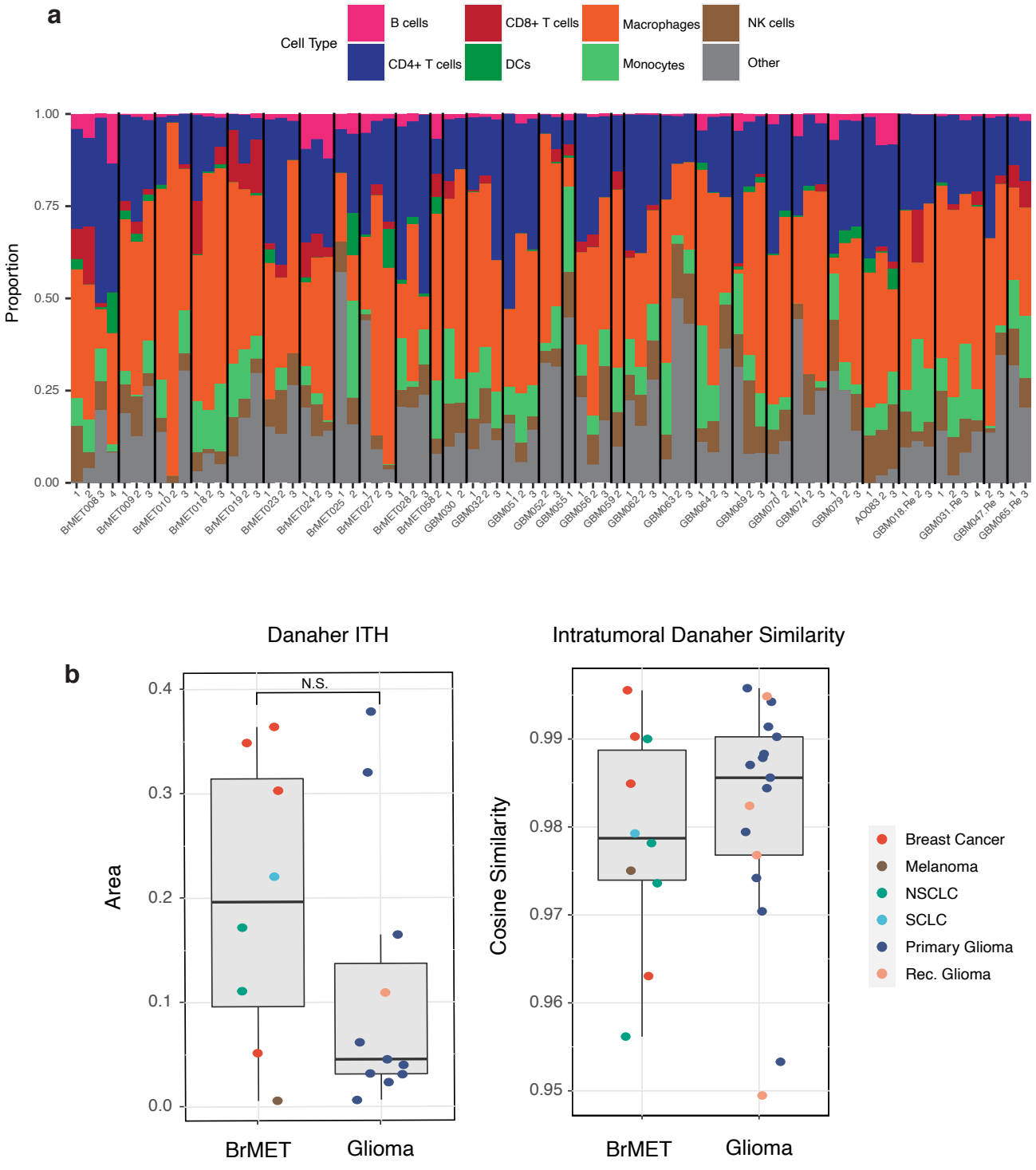

Supplementary Fig. 8: Immune microenvironment profiling and intratumoral heterogeneity. **a,** Simplified CIBERSORT (see Methods) output estimating abundance for each immune cell type for each tumor sample in cohort. **b,** Quantification of immune intratumoral heterogeneity or similarity through either the area encompassed by regions from each tumor in PC1-PC2 space (left) or an intratumoral pairwise cosine similarity metric on vectors composed of the Danaher immune scores for each region (right).

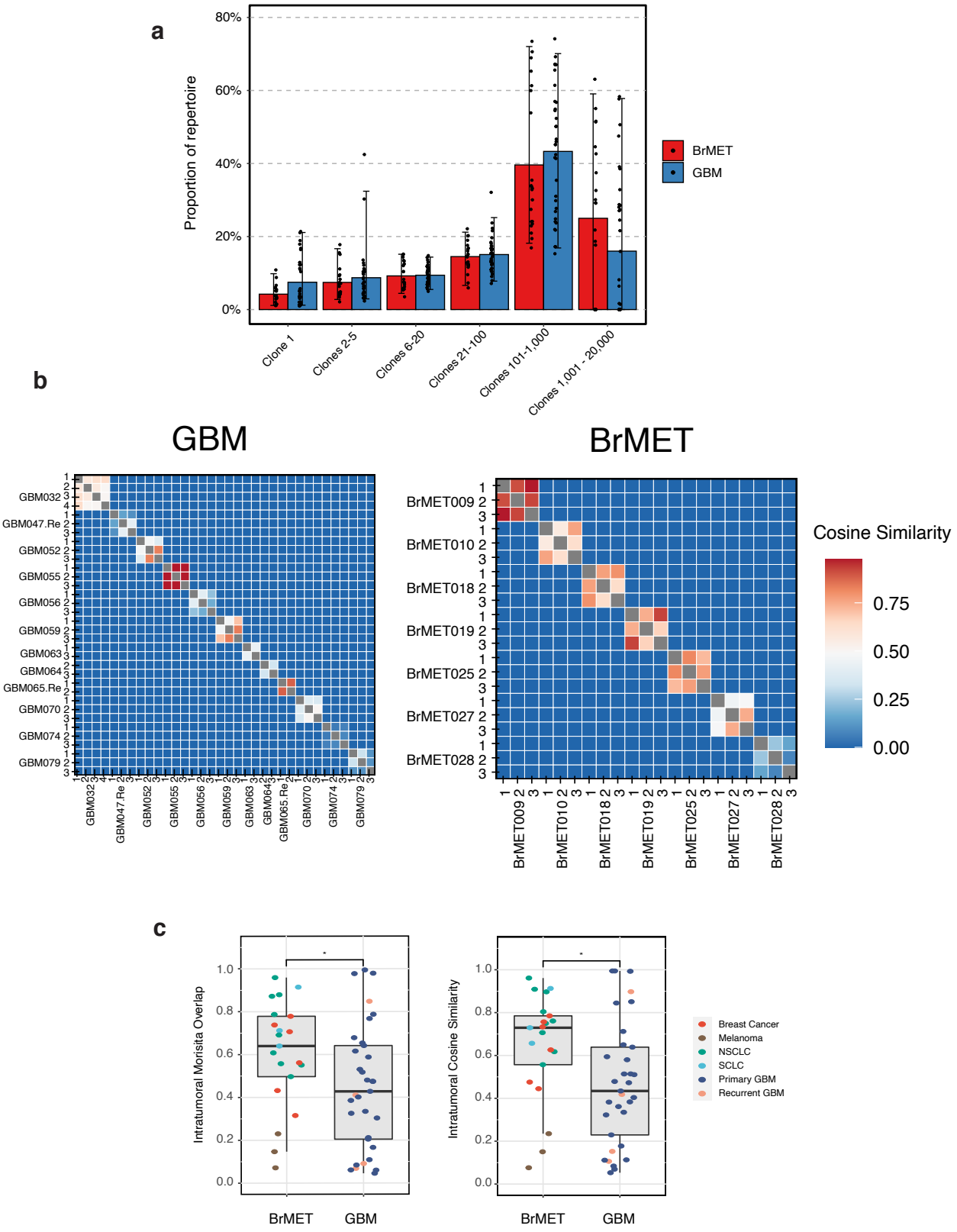

Supplementary Fig. 9: Intratumoral T cell repertoire heterogeneity. a, The proportion of the T cell repertoire for each sample comprised of clones within a given clonotype group when clones are ranked in descending order of frequency. **b,** Quantification of TCR intratumoral heterogeneity by calculation of the cosine similarity (see Methods) between pairs of distinct tumor regions in either GBM (left) or BrMETs (right). Values range from 0 (indicating no similarity) to 1 (identical TCR repertoires). **c,** Comparison of intratumoral T cell repertoire similarity between GBM and BrMETs via either Morisita overlap (left) or cosine similarity (right). Each data point represents the pairwise comparison between regions from the same tumor. Significance determined by unpaired t-test. *p<0.05.

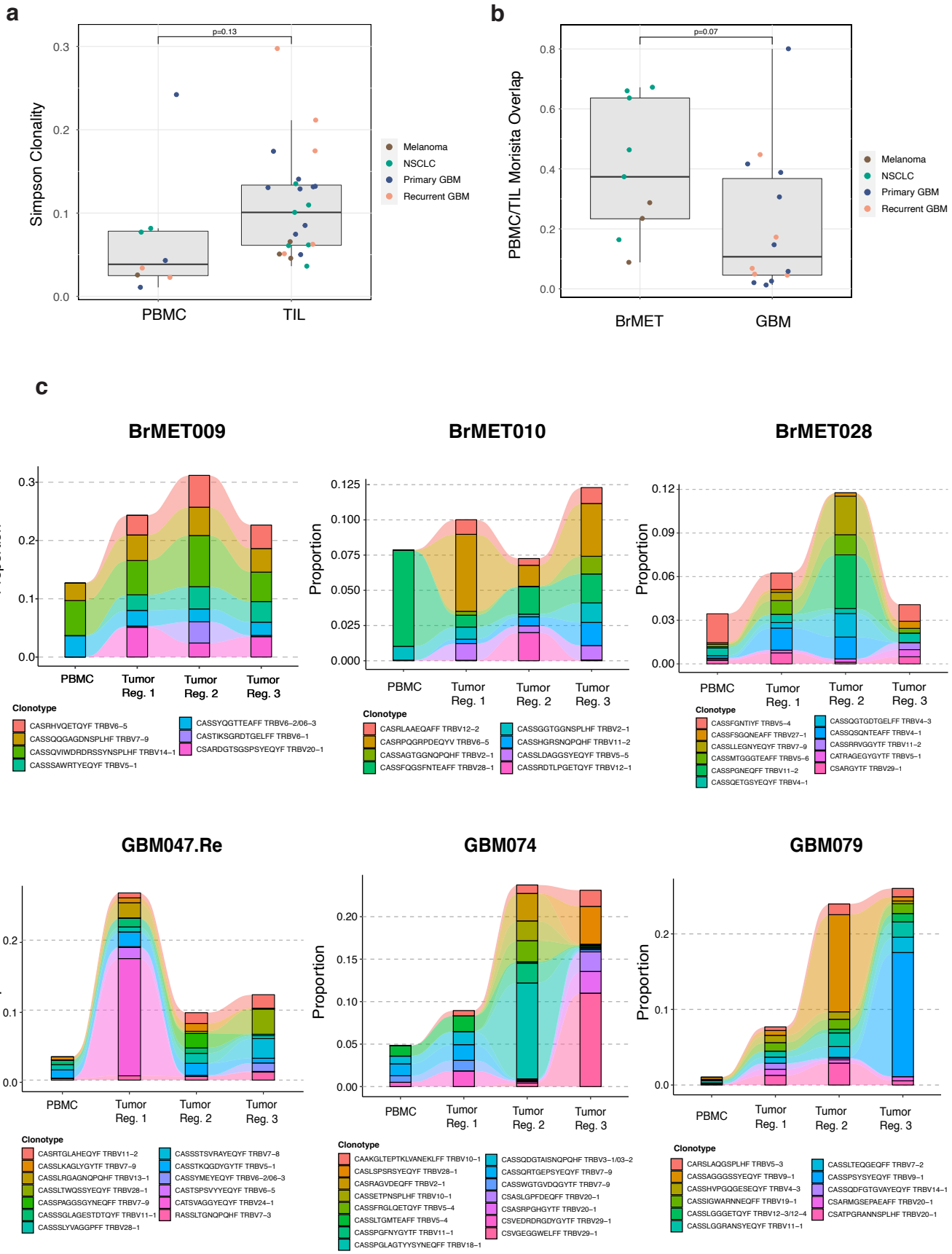

Supplementary Fig. 10: Clonality and similarity of peripheral blood T cell repertoire. a, Comparison of T cell repertoire Simpson clonality between peripheral blood and matched TIL. **b,** Quantification of TCR similarity between peripheral blood and matched TIL through calculation of the Morisita overlap (see Methods). Values range from 0 (indicating no similarity) to 1 (identical TCR repertoires). **c,** Alluvial plots tracking the frequencies of the top 5 clonotypes from within each region of the tumor. Each clonotype is defined below the associated plot by the amino acid sequence of its CDR3 and the V gene used.

BrMET009

PBMC

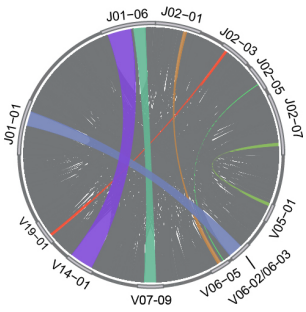

Tumor Reg. 1

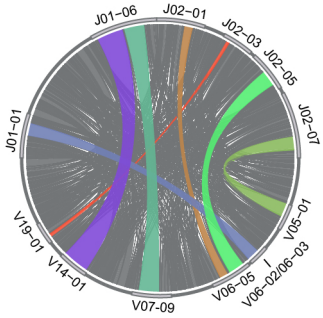

Tumor Reg. 2

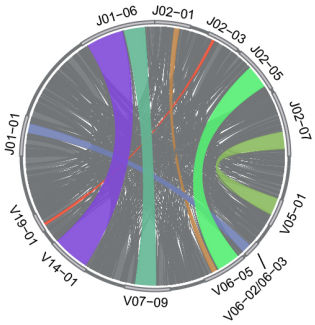

Tumor Reg. 3

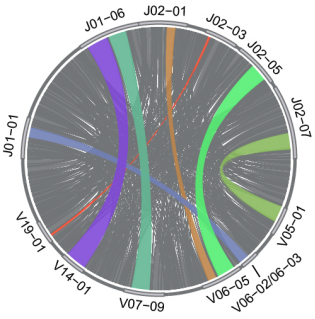

GBM047.Re

PBMC

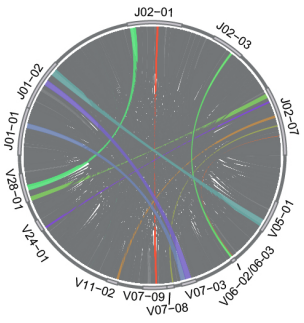

Tumor Reg. 1

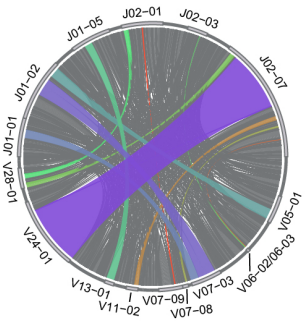

Tumor Reg. 2

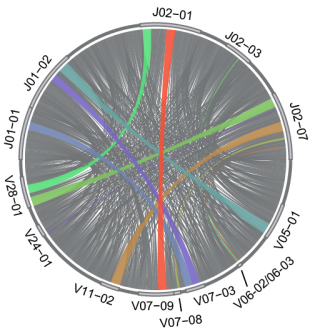

Tumor Reg. 3

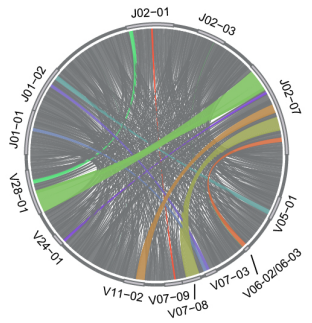

GBM074

PBMC

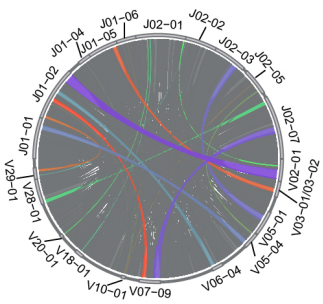

Tumor Reg. 1

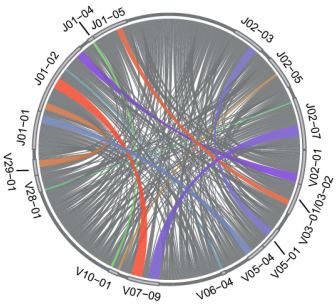

Tumor Reg. 2

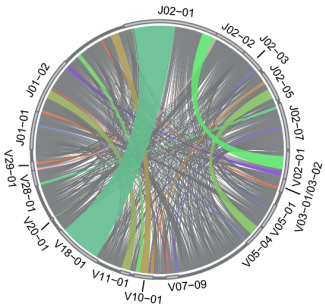

Tumor Reg. 3

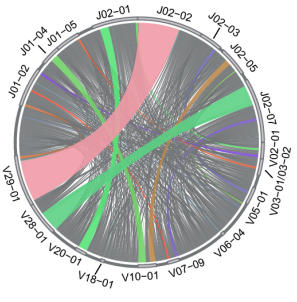

Supplementary Fig. 11: Distribution of T cell repertoire V-J usage. Modified circos plots displaying the prominent V-J gene combinations within select tumors and matched peripheral blood. The frequency of a given V or J gene segment within the repertoire is represented by its arc length along the circle, while the width of the connection between a given V-J pair corresponds to the frequency of that combination. Within each patient, the top 5 V-J pairs within any one region are highlighted across all matched samples. All plots correspond to V-J usage among TCR β chain sequences.

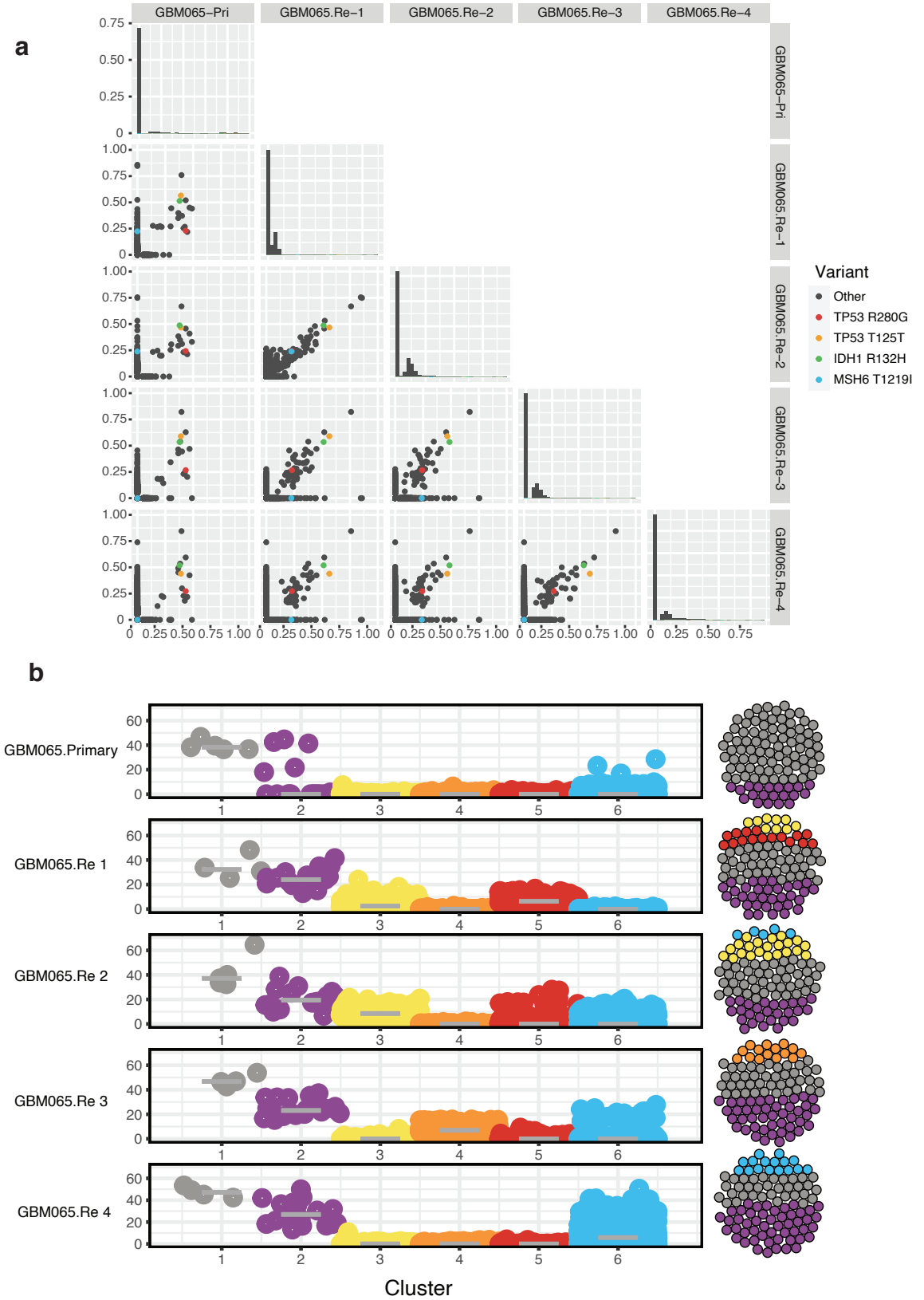

Supplementary Fig. 12: Clonal landscape of GBM065. a, Pairwise VAF comparisons for GBM065 primary and recurrent samples. **b**, Clonal architecture of GBM065 primary and recurrent tumor samples generated by ClonEvol. Overall clonal composition of each sample is represented by fraction of shaded spheres. .

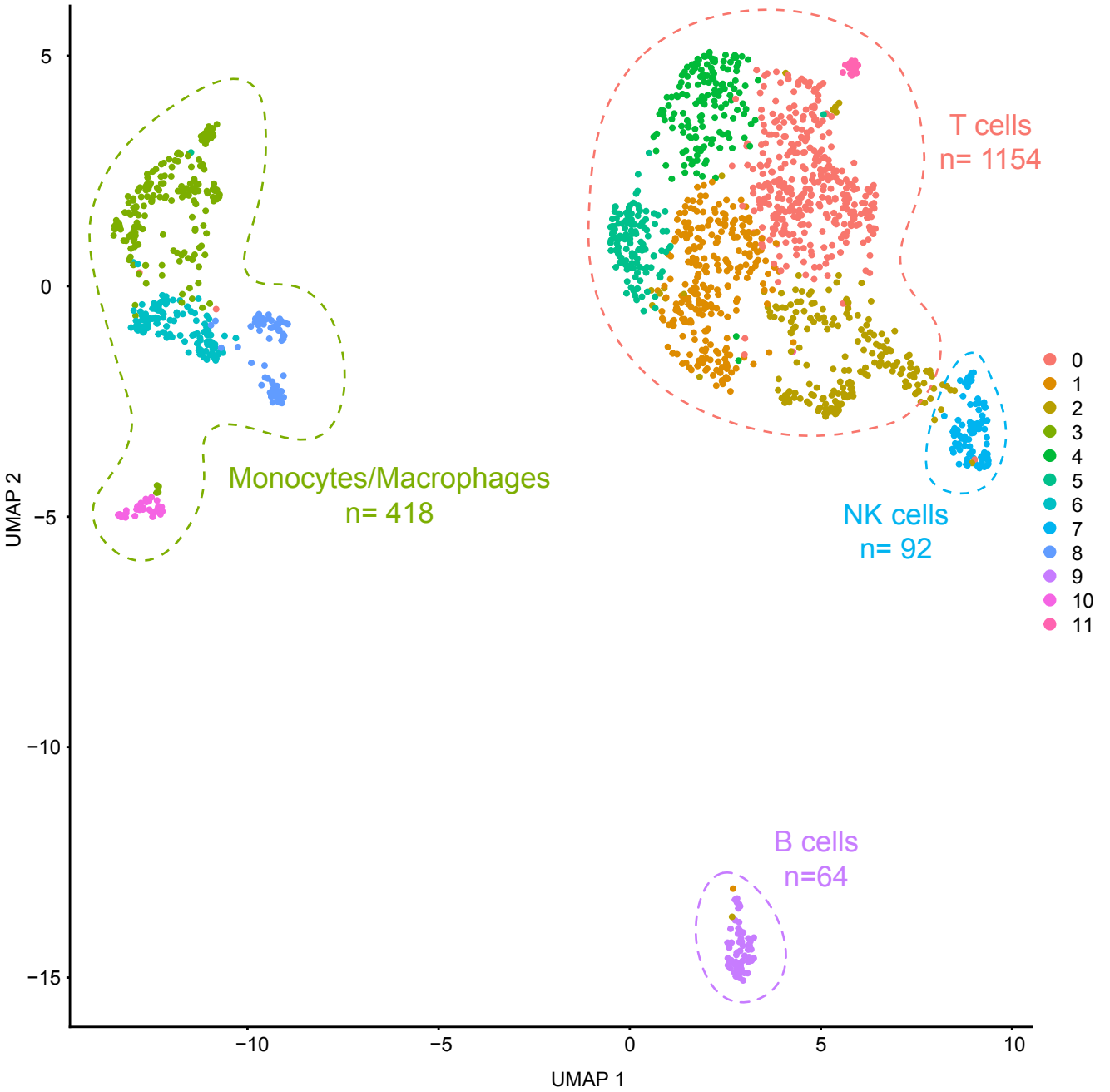

Supplementary Fig. 13: Single-cell RNA-seq on hypermutated recurrent GBM. Uniform manifold approximation and projection (UMAP) visualization of all cells from the patient sample GBM065.Re (n= 1,728). Major cell clusters, marked by dashed outlines, were identified using previously reported cell markers. Cell clusters were generated via unsupervised graph-based clustering of cells with a resolution of 0.8.